A LETTERS JOURNAL EXPLORING THE FRONTIERS OF PHYSICS

OFFPRINT

Tune the "rainbow" trapped in a multilayered waveguide

QING HU, DI-HU XU, RU-WEN PENG, YU ZHOU, QIAN-LI YANG and MU WANG

EPL, **99** (2012) 57007

A Letters Journal Exploring the Frontiers of Physics

September 2012

EPL, **99** (2012) 57007
doi: 10.1209/0295-5075/99/57007

www.epljournal.org

Tune the "rainbow" trapped in a multilayered waveguide

Qing Hu, Di-Hu Xu, Ru-Wen Peng[a], Yu Zhou, Qian-Li Yang and Mu Wang[b]

National Laboratory of Solid State Microstructures and Department of Physics, Nanjing University Nanjing 210093, China

received 14 June 2012; accepted in final form 8 August 2012
published online 11 September 2012

PACS 78.67.Pt – Multilayers; superlattices; photonic structures; metamaterials
PACS 61.44.Br – Quasicrystals
PACS 42.70.Qs – Photonic bandgap materials

Abstract – The "rainbow", where the light waves with different frequencies separate spatially, is confined in a self-similar waveguide with a hollow core coated by a coaxial dielectric/liquid-crystal multilayer. Due to the intrinsic self-similar furcation of the system, multiple transmission bands emerge in the photonic band structure, a "rainbow" is trapped as cladding modes in the waveguide. Both photonic bands and transmission modes can be tuned by changing temperature, hence the "rainbow" changes the colors in the waveguide. This effect can be applied in designing temperature-dependent integrated photonic devices, such as tunable on-chip spectroscopy, on-chip color-sorters, and photon sorters for spectral imaging.

Introduction. – Photons are desired to act as carriers in information transfer thus they need be artificially manipulated [1,2]. Traditionally, optical waveguides are employed to confine and guide the light waves, which have become the key components of global telecommunicated networks [3]. In the past decade, it was demonstrated that both photonic crystal waveguides [4–6] and cylindrical Bragg waveguides are capable of trapping light in their cores [7–10], which attracted much interest. In recent years, several novel schemes have been proposed to trap, store and release light waves. For example, a photonic crystal with defects has been used to localize and release photons [11], and metamaterials are proposed to trap "rainbow" at terahertz [12] and telecommunication [13] frequencies. Very recently, it has been predicted that a quasiperiodic dielectric waveguide is also able to trap the "rainbow" [14]. All these features offer prospective applications in integrated photonic devices, such as on-chip spectroscopy and imaging devices [15–17].

In technical applications, it is worthwhile to tune the devices by external fields. It is well known that liquid crystal [18,19] is one of the most important optical materials and has been widely applied in daily life, mainly because its optical properties can be tuned thermally [20], optically [21] and electrically [22,23], respectively. Consequently, some liquid crystal devices, such as electrically controlled photonic bandgap fibers and polarimeters [24, 25], have been achieved. Inspired by these facts, here we demonstrate a self-similar waveguide infiltrated by liquid crystal to achieve tunable "rainbow trapping". Due to the self-similar furcation feature, we show that the multiple transmission bands appear in the photonic band structure, a "rainbow" is trapped as cladding modes in the waveguide. Furthermore, by changing the temperature, the refractive index of the liquid crystal varies, thereafter, both the photonic bands and the transmission modes are tuned. As a result, the "rainbow" in the waveguide significantly changes its color and pattern when the temperature is changed.

"Rainbow" trapped in a self-similar liquid-crystal/dielectric waveguide. – The self-similar liquid-crystal/dielectric waveguide (SLDW) is designed with a hollow core surrounded by a coaxial Thue-Morse multilayer. The Thue-Morse sequence is one of the well-known examples in one-dimensional quasiperiodic structures [26], and it contains two building blocks A and B and can be produced by repeating application of the substitution rules $A \to AB$ and $B \to BA$ [27–29]. In the SLDW, the coaxial Thue-Morse multilayer consists of two building blocks: A is the dielectric with refractive index n_A and B is the liquid crystal, and their thicknesses are d_A and d_B, respectively, as shown in fig. 1. In the following calculations, the radius of the hollow core is set as $R_0 = 3a$, the refractive index as $n_A = 4.6$, and the

[a]E-mail: rwpeng@nju.edu.cn
[b]E-mail: muwang@nju.edu.cn

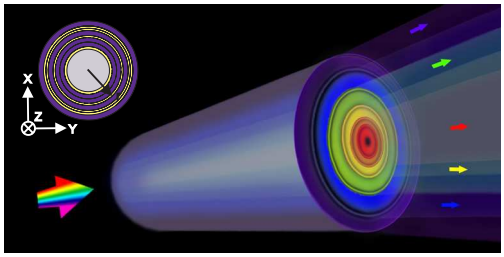

Fig. 1: (Color online) The schematic rainbow trapping in SLDW and the cross section of the waveguide (inset). In the SLDW, a hollow core (refractive index $n_0 = 1$) is surrounded by a coaxial Thue-Morse multilayer consisting of two building blocks A (yellow layer) and B (blue layer), where A is for dielectric and B is for liquid crystal, respectively.

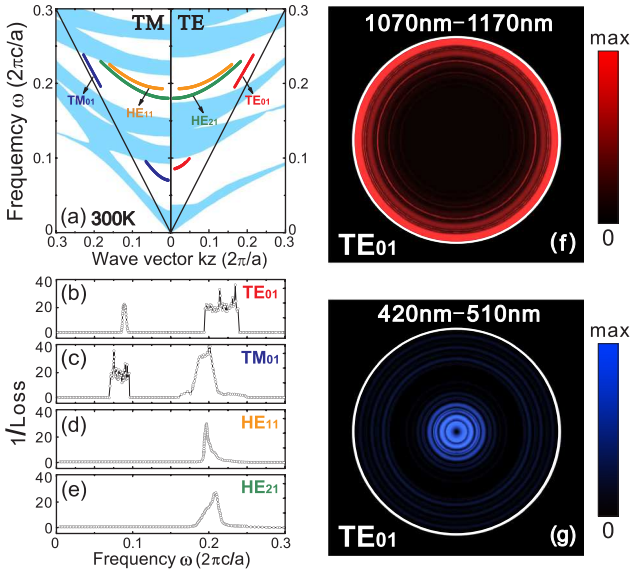

Fig. 2: (Color online) (a) The photonic band structure for both TE and TM polarizations and the propagating modes in SLDW with three generations at the temperature $T = 300\,\mathrm{K}$. The low-frequency modes are dotted: the red is for TE_{01}, the blue is for TM_{01}, the orange is for HE_{11}, and the green is for HE_{21}. Higher modes are not shown here. The black solid line denotes the light line in air. The reciprocal of the loss (1/loss) as a function of frequency for different modes: (b) TE_{01}, (c) TM_{01}, (d) HE_{11}, and (e) HE_{21}, respectively. Here the characterized size of the SLDW is $a = 100\,\mathrm{nm}$, thereafter, the SLDW works at optical frequency. (f)–(g) The electric-field time-average energy density distributions of TE_{01} mode.

thickness as $d_A = 0.4a$ and $d_B = 1.2a$, respectively. Here a is the characterized size of the SDW, which corresponds to the operation wavelength of the waveguide. For example, the waveguide can operate at optical frequency if $a = 100\,\mathrm{nm}$. In order to make the calculations more realistic, we take a high-birefringence liquid crystal called as mixture UCF-35 [20] as an example, where the refractive index is temperature-dependent. Actually the molecules of the liquid crystal UCF-35 can be aligned naturally [20]. Here we assume the directions of the molecules are along the axis of the waveguide, which leads to distinct longitudinal and transverse refractive indices, $n_e(T)$ and $n_o(T)$, respectively.

By applying the transfer matrix method to cylindrical coordinate system [30] and considering the optical birefringence, photonic band structures and propagating modes in the SLDW can be numerically calculated. Figure 2(a) illustrates the photonic band structure and the propagating modes in the SLDW, which contains the cladding Thue-Morse multilayer with three generations at the temperature $T = 300\,\mathrm{K}$. The Thue-Morse multilayer with three generations includes 8 layers. As shown in fig. 2(a), there exist several frequency regions (marked in blue), where the light transmits throughout the cladding layers; whereas there also exist the frequency regions (marked in white), where the light is confined in the SLDW, known as the photonic band gaps (PBGs). Here the PBGs are for both transverse electric (TE) and transverse magnetic (TM) polarizations. Comparing with the periodic dielectric waveguides [8–10], more PBGs exist in the SLDW. Note that usually a small aperiodic structure presents obvious differences with respect to the periodic one. For example, according to the calculation, the Thue-Morse multilayer with 2 generations (4 layers) has one more photonic band than the periodic one. These multiple PBGs originate from the self-similarity in the SLDW and possess the furcation feature, which makes it possible to select the propagating modes in the waveguide.

The propagating modes in the SLDW possess several unique features. First, there exist several types of modes (as shown in fig. 2(a)), such as the polarization modes TE_{01} and TM_{01}, and the hybrid modes HE_{11} and HE_{21} at the low-frequency regime. Second, the propagating modes are separated by the PBGs. For example, TE_{01} modes exist in two frequency ranges as $\omega/\omega_0 = 0.035$–0.100, and 0.175–0.240, respectively ($\omega_0 = 2\pi c/a$), suggesting that the propagating modes are frequency-selective in the waveguide. Third, the frequency ranges for different modes may overlap. For instance, in the frequency range of $\omega/\omega_0 = 0.175$–0.240, there exist four types of modes: TE_{01}, TM_{01}, HE_{11} and HE_{21}. This means that the SLDW can be used as a multimode waveguide. In order to quantify the transmission performance of the waveguide, we have investigated the loss of light in the SLDW. The loss of the propagating mode is defined as the ratio of the radial-outgoing power to its forward-propagating power in the waveguide [14]. As illustrated in fig. 2(b)–(e), it is obvious that the modes of TE_{01}, TM_{01}, HE_{11} and HE_{21} propagate in the SLDW at the frequency regions, which exactly correspond to their transmission regions in fig. 2(a). The low losses indicate good transmission performance of the modes in the waveguide. It is noteworthy that the electromagnetic fields for different modes are spatially separated in different cladding layers of the SLDW. As illustrated in fig. 2, the lights with the wavelength of $\lambda =$ 1070 nm–1170 nm are trapped near the outermost cladding

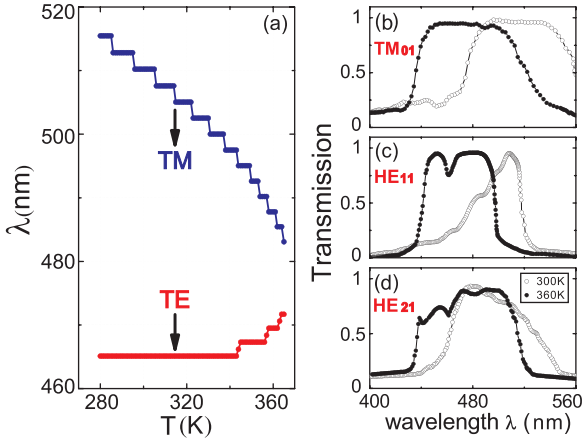

Fig. 3: (Color online) (a) The central wavelength of the photonic bandgap at visible frequencies in the SLDW with three generations as a function of temperature for transverse electric (TE, shown in red) and transverse magnetic (TM, shown in blue), respectively. (b)–(d) The transmission efficiency of the modes in the SLDW as a function of wavelength at different temperatures: (b) TM_{01}, (c) HE_{11}, and (d) HE_{21}, respectively. The temperatures are $T = 300\,\mathrm{K}$ and $T = 360\,\mathrm{K}$, respectively.

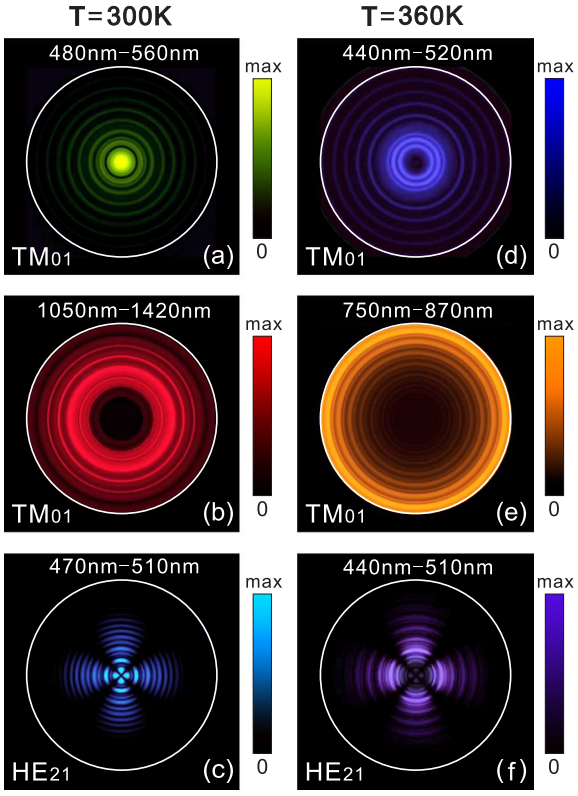

Fig. 4: (Color online) The electric-field time-average energy density distributions for the modes in the SLDW at different temperatures: (a)–(b) TM_{01} and (c) HE_{21} at the temperature $T = 300\,\mathrm{K}$; (d)–(e) TM_{01} and (f) HE_{21} at the temperature $T = 360\,\mathrm{K}$.

layers (fig. 2(f)); whereas the lights with $\lambda = 420$–$510\,\mathrm{nm}$ appear in the core layer and in the first few cladding layers (fig. 2(g)). From this point of view, a "rainbow" is trapped in the SLDW.

Tune the "rainbow" by altering the temperature. – Due to the fact that the refractive index of the liquid crystal UCF-35 is temperature-dependent, the propagating modes and the trapped "rainbow" can be tuned by altering the temperature in SLDW. On the one hand, the PBGs of the SLDW can be tuned by changing the temperature. Figure 3(a) illustrates the central wavelength of the PBG in the visible region as a function of temperature for TE and TM polarizations, respectively. As temperature increases, the central wavelength of the PBG decreases dramatically for TM, yet it increases slightly for TE. This difference originates from the fact that the anisotropic refractive indices of the liquid crystal in the SLDW have different temperature responses. Therefore, it is possible to tune PBGs by both temperature and polarization. On the other hand, the propagating modes in the SLDW can also be tuned by temperature. We define the transmission efficiency of the light as the ratio between the power confined inside the waveguide with a length l and its total input power, *i.e.*,

$$T(\omega) = \frac{\int_0^l \mathrm{d}z \int_0^{2\pi} \mathrm{d}\phi \int_0^R P(r,\phi,z) r \mathrm{d}r}{P_0 \pi R^2 l}, \qquad (1)$$

where $P(r,\phi,z)$ is the time-average electromagnetic energy density in the waveguide, and P_0 is the initially input energy density; R stands for the outermost radius of the waveguide. For the modes of TM_{01}, HE_{11}, and HE_{21}, we calculate their transmission efficiencies as a function of wavelength at temperature $T = 300\,\mathrm{K}$ and $T = 360\,\mathrm{K}$, respectively, as shown in figs. 3(b)–(d). It is obvious that the high transmission region at the visible wavelengths has a blue shift when the temperature increases. For instance, when the temperature changes from 300 K to 360 K, the TM_{01} mode moves from 480 nm–560 nm to 440 nm–520 nm (fig. 3(b)), the HE_{11} mode moves from 480 nm–520 nm to 440 nm–500 nm (fig. 3(c)), whereas the HE_{21} mode moves from 470 nm–510 nm to 440 nm–510 nm (fig. 3(d)). For the other wavelengths, the shifts also exist. Therefore, the propagating mode is indeed tunable by temperature in the SLDW.

The temperature-dependent propagating modes can lead to a tunable "rainbow" trapping in the SLDW. To confirm this further, we calculate the energy density distribution of the electric field for different modes in the SLDW at different temperature. As indicated in fig. 4, different modes are spatially separated in the waveguide when the temperature is fixed. While for the same mode, the spatial distribution of the electromagnetic fields changes significantly when the temperature is changed. The pattern enlarges with the blue shift of the transmission region at high temperature. For example, for the TM_{01} mode, the light with $\lambda = 480\,\mathrm{nm}$–$560\,\mathrm{nm}$ is trapped mainly in the core layer at $T = 300\,\mathrm{K}$ (fig. 4(a)). However, when

the temperature is increased to $T = 360\,\mathrm{K}$, the mode is shifted to $\lambda = 440\,\mathrm{nm}$–$520\,\mathrm{nm}$, and is trapped in the first few cladding layers (fig. 4(d)). In addition, the light with $\lambda = 1050\,\mathrm{nm}$–$1420\,\mathrm{nm}$ is trapped in the first few cladding layers at the temperature $T = 300\,\mathrm{K}$ (fig. 4(b)), by increasing temperature to $T = 360\,\mathrm{K}$, it moves to $\lambda = 750\,\mathrm{nm}$–$870\,\mathrm{nm}$, and is then trapped near the outermost cladding layers (fig. 4(e)). Let us take the HE_{21} mode as a further example. The light with $\lambda = 470\,\mathrm{nm}$–$510\,\mathrm{nm}$ is trapped between the core layer and the middle cladding layers at $T = 300\,\mathrm{K}$ (fig. 4(c)); yet when the temperature is increased to $T = 360\,\mathrm{K}$, the mode is shifted to $\lambda = 440\,\mathrm{nm}$–$510\,\mathrm{nm}$, which is confined near the middle cladding layers (fig. 4(f)).

Summary. – We presented the frequency selection and the spatial separation of light in a SLDW with a hollow core and a coaxial Thue-Morse liquid-crystal/dielectric multilayer. Due to the self-similar furcation feature, multiple transmission bands appear in the photonic band structure, a "rainbow" is trapped as cladding modes in the waveguide. By changing the temperature, both photonic bands and propagation modes can be tuned. Consequently, the "rainbow" in the waveguide can change color and pattern. We expect that this effect can be applied to designing temperature-tuned integrated photonic devices, such as a temperature sensor, temperature-dependent switch on chip, tunable on-chip spectroscopy, and photon sorters for spectral imaging.

* * *

This work was supported by the Ministry of Science and Technology of China (Grant Nos. 2012CB921502 and 2010CB630705), the National Science Foundation of China (Grant Nos. 11034005, 61077023, 50972057 and 11021403), and partly by Jiangsu Province (BK2008012) and the Ministry of Education of China (20100091110029).

REFERENCES

[1] Foresi J. S., Villeneuve P. R., Ferrera J., Thoen E. R., Steinmeyer G., Fan S., Joannopoulos J. D., Kimerling L. C., Smith Henry I. and Ippen E. P., *Nature*, **390** (1997) 143.
[2] Zi J., Wan J. and Zhang C., *Appl. Phys. Lett.*, **73** (1998) 2084.
[3] Miller S. E. and Chynoweth A. G., *Optical Fiber Telecommunications* (Academic Press, New York) 1979.
[4] Russell P., *Science*, **299** (2003) 358.
[5] Knight J. C., *Nature*, **424** (2003) 847.
[6] Skibina J. S., Iliew R., Bethge J., Bock M., Fischer D., Beloglasov V. I., Wedell R. and Steinmeyer G., *Nat. Photon.*, **2** (2008) 679.
[7] Yeh P., Yariv A. and Marom E., *J. Opt. Soc. Am.*, **68** (1978) 1196.
[8] Ibanescu M., Fink Y., Fan S., Thomas E. L. and Joannopoulos J. D., *Science*, **289** (2000) 415.
[9] Ibanescu M., Johnson S. G., Soljacic M., Joannopoulos J. D. and Fink Y., *Phys. Rev. E*, **67** (2003) 046608.
[10] Temelkuran B., Hart S. D., Benoit G., Joannopoulos J. D. and Fink Y., *Nature*, **420** (2002) 650.
[11] Noda S., Chutinan A. and Imada M., *Nature*, **407** (2000) 608.
[12] Tsakmakidis K. L., Boardman A. D. and Hess O., *Nature*, **450** (2007) 397.
[13] Gan Q., Ding Y. J. and Bartoli F. J., *Phys. Rev. Lett.*, **102** (2009) 056801.
[14] Hu Q., Zhao J. Z., Peng R. W., Gao F., Zhang R. L. and Wang M., *Appl. Phys. Lett.*, **96** (2010) 161101.
[15] Barnes W. L., Dereux A. and Ebbesen T. W., *Nature*, **424** (2003) 824.
[16] Lal S., Link S. and Halas N. J., *Nat. Photon.*, **1** (2007) 641.
[17] Laux E., Genet C., Skauli T. and Ebbesen T. W., *Nat. Photon.*, **2** (2008) 161.
[18] Chandrasekhar S., *Liquid Crystals* (Cambridge University Press, Cambridge, England) 1992.
[19] de Gennes P. G. and Prost J., *The Physics of Liquid Crystals* (Clarendon Press Oxford, England) 1993.
[20] Li J., Gauza S. and Wu S. T., *J. Appl. Phys.*, **96** (2004) 19.
[21] Alkeskjold T. T., Laegsgaard J., Bjarklev A., Hermann D. S., Anawati, Broeng J., Li J. and Wu S. T., *Opt. Express*, **12** (2004) 5857.
[22] Haakestad M. W., Alkeskjold T. T., Nielsen M. D, Scolari L., Riishede J., Engan H. E. and Bjarklev A., *IEEE Photon. Technol. Lett.*, **17** (2005) 819.
[23] Busch K. and John S., *Phys. Rev. Lett.*, **83** (1999) 2.
[24] Weirich J., Laegsgaard J., Scolari L., Wei L., Alkeskjold T. T. and Bjarklev A., *Opt. Express*, **17** (2009) 4442.
[25] Alkeskjold T. T. and Bjarklev A., *Opt. Lett.*, **32** (2007) 1707.
[26] Macia E., *Rep. Prog. Phys.*, **75** (2012) 036502.
[27] Godreche C. and Luck J. M., *J. Phys. A*, **23** (1990) 3769.
[28] Qiu F., Peng R. W., Huang X. Q., Liu Y. M., Wang M., Hu A. and Jiang S. S., *Europhys. Lett.*, **63** (2003) 853.
[29] Qiu F., Peng R. W., Huang X. Q., Hu X. F., Wang M., Hu A, Jiang S. S and Feng D., *Europhys. Lett.*, **68** (2004) 658.
[30] Xu Y., Ouyang G. X., Lee R. K. and Yariv A., *J. Waveguide Technol.*, **20** (2002) 0733.